ENVIRONMENTAL RESEARCH
COMMUNICATIONS

INCLUSIVE PUBLISHING
TRUSTED SCIENCE

Part of the
ENVIRONMENTAL RESEARCH
SERIES

PURPOSE-LED
PUBLISHING™

PAPER • **OPEN ACCESS**

Source apportionment and human health risk assessment of PAHs and PCBs in greenhouse soil systems

To cite this article: Güray Doğan *et al* 2026 *Environ. Res. Commun.* **8** 085023

View the article online for updates and enhancements.

You may also like

- Distribution and the use of diagnostic ratios for source investigation in urban soils of the Yenagoa City, Bayelsa State, Nigeria
Kaywood Elijah Leizou
- Determination of Polycyclic Aromatic Hydrocarbons in Selected Soils from Al-Diwaniyah governorate, Iraq-Case Study
Tania S. Kadhim and Faiq F. Karam
- Concentration of some Polycyclic Aromatic Hydrocarbons in soil samples of Kirkuk province, Iraq
Yasin H Aoeed, Awaz B Mohammed and Attalah M. Hameed

This content was downloaded from IP address 194.27.186.93 on 14/09/2026 at 22:14

Environmental Research Communications

Check for updates

OPEN ACCESS

RECEIVED
6 May 2026

REVISED
29 July 2026

ACCEPTED FOR PUBLICATION
6 August 2026

PUBLISHED
17 August 2026

Original content from this work may be used under the terms of the Creative Commons Attribution 4.0 licence.

Any further distribution of this work must maintain attribution to the author(s) and the title of the work, journal citation and DOI.

PAPER

Source apportionment and human health risk assessment of PAHs and PCBs in greenhouse soil systems

Güray Doğan, Ahmet Mustafa Tepe*, Ebru Nur Dokumacı and Bihter Olgun

Department of Environmental Engineering, Akdeniz University, Antalya 07058, Türkiye
* Author to whom any correspondence should be addressed.

E-mail: ahmettepe@akdeniz.edu.tr

Keywords: PAHs, PCBs, soil pollution, source apportionment, greenhouse farming, risk assessment

Supplementary material for this article is available online

Abstract

Intensive greenhouse farming creates distinct enclosed microclimates that can exacerbate the accumulation of persistent organic pollutants in agricultural soils. The primary objectives of this study were to quantify 16 polycyclic aromatic hydrocarbons (PAHs) and 12 polychlorinated biphenyls (PCBs) in tomato-cultivated greenhouse soils in Antalya, Turkiye, to apportion their emission sources, and to explicitly evaluate the influence of greenhouse cover materials (glass vs polyethylene plastic) and seasonal variations on pollutant dynamics. Furthermore, the study aimed to conduct a multi-pathway occupational health risk assessment specifically tailored for greenhouse workers. A total of 100 soil samples were collected across two campaigns (autumn and winter) from 50 greenhouses and 5 reference sites. Following GC/MS quantification, source apportionment was performed using EPA PMF 5.0, and human health risks were estimated via United States Environmental Protection Agency deterministic models. Results indicated that total PAH concentrations were generally higher in glass greenhouses due to limited UV-driven photodegradation, whereas PCB levels showed stronger inter-compound correlations under plastic covers governed by distinct ventilation practices. Positive matrix factorization modeling identified five PAH sources, dominated by diesel combustion (33%), and three PCB sources, primarily driven by atmospheric transport and commercial mixtures (60%). Occupational health assessments revealed that the incremental lifetime cancer risk for PAHs (6.45×10^{-5}) and the non-carcinogenic Hazard Index for PCBs (1.30×10^{-3}) remained within acceptable regulatory safety limits. However, dermal contact emerged as the overwhelmingly dominant exposure pathway (accounting for ∼75% of the total risk), highlighting the critical need for targeted occupational hygiene practices in enclosed agricultural environments.

1. Introduction

Greenhouses are controlled environments designed to optimize conditions for crop cultivation by maintaining stable internal microclimates irrespective of external environmental fluctuations. This controlled system plays a significant role in modern agriculture, allowing year-round production and enhancing crop yields (Dorais *et al* 2000). In regions with favorable climates, such as Antalya, Turkiye, greenhouses are a vital component of the agricultural sector, contributing substantially to the local economy by providing a consistent supply of fresh produce (Ceylan *et al* 2018). Antalya's Mediterranean climate, characterized by warm temperatures and long hours of sunlight, makes it particularly suited to greenhouse-based cultivation (Zaimoglu and Baytorun 2018, Karaca 2023).

Despite their benefits, greenhouse systems are not without environmental concerns. The accumulation of persistent organic pollutants (POPs), such as polycyclic aromatic hydrocarbons (PAHs) and polychlorinated biphenyls (PCBs), in greenhouse soils presents significant environmental and public health

© 2026 The Author(s). Published by IOP Publishing Ltd

risks. POPs are highly resistant to environmental degradation and can persist in soil for extended periods. They have been linked to adverse health effects, including carcinogenicity, mutagenicity, and teratogenicity, which pose long-term risks to both ecosystems and human populations (Tsai 2010; X. Zhang *et al* 2021). The persistence of these pollutants enables long-range atmospheric transport, resulting in their dissemination far beyond their initial source regions (Xing *et al* 2005, Kilunga *et al* 2017).

PAHs are a class of organic compounds formed during the incomplete combustion of organic matter, including fossil fuels, coal, oil, gas, and biomass. Natural sources such as volcanic eruptions and wildfires also contribute to their presence in the environment (Ravindra *et al* 2008). Owing to their lipophilic properties, PAHs have a high affinity for soil particles, leading to their accumulation in agricultural soils, including those in greenhouse systems (D. Wilcke 2007, Wang *et al* 2018).

On the other hand, *PCBs* are synthetic organic chemicals once widely used in industrial applications, particularly as dielectric and coolant fluids in transformers and capacitors (Hu *et al* 2011, Jahnke and Hornbuckle 2019). Although PCBs were banned in most countries in the late 20th century due to their hazardous nature, their persistence in the environment and bioaccumulation in the food chain continue to make them a global environmental concern (Yao *et al* 2014). Contamination of soils with PCBs can occur via atmospheric deposition, runoff from contaminated sites, and leaching (Combi *et al* 2016).

Greenhouses have become a vital component of modern agriculture, providing controlled environments that enable year-round cultivation. The type of cover material used, typically glass or plastic, plays a crucial role in the overall effectiveness of greenhouses. Glass greenhouses are traditionally favored for their durability and ability to transmit high levels of light, fostering optimal growth conditions for many crops. However, plastic-covered greenhouses, which often use materials such as polyethylene or polycarbonate, have gained popularity because of their low cost, flexibility, and ease of installation. The choice of cover material significantly impacts a greenhouse's energy efficiency, microclimate, and environmental footprint. For instance, plastic covers tend to trap more heat, reducing the need for artificial heating, but may degrade over time, contributing to plastic waste if not properly managed (von Elsner *et al* 2000).

The environmental implications of selecting either glass or plastic for greenhouse covers extend beyond the immediate agricultural benefits. Glass greenhouses, while longer lasting, require more initial energy inputs during construction and can lead to higher long-term energy costs due to heat loss (Maraveas 2019). However, plastic greenhouses, though more energy-efficient in terms of heat retention, pose challenges related to waste management and the potential leaching of chemicals from degraded plastic materials into the soil (Scarascia-Mugnozza *et al* 2011). Studies have shown that the type of cover material can influence the accumulation of pollutants in greenhouse soils. For instance, plastic materials can lead to higher concentrations of volatile organic compounds and POPs such as PAHs and PCBs because of their interactions with the greenhouse environment. As greenhouses continue to evolve with technological advancements, selecting appropriate cover materials must balance crop productivity, environmental sustainability, and long-term ecological impacts.

Identifying the sources and pathways of these pollutants in greenhouse soils is crucial for mitigating their impacts. Positive matrix factorization (PMF), a multivariate receptor model, is a widely accepted statistical technique for source apportionment in complex environmental matrices (Paatero and Tapper 1994). By analyzing the chemical composition of soil samples, PMF can distinguish between various pollution sources and provide quantitative estimates of their contributions (Norris *et al* 2014). This methodology has been successfully applied to determine the sources of PAHs and PCBs in numerous environmental studies, including those focusing on soil contamination (Chai *et al* 2017, Ciarkowska *et al* 2022, Li *et al* 2023, Zhang *et al* 2023).

Although receptor models have been widely applied to apportion sources of POPs across various open environments, the distinct dynamics and the occupational health implications of these contaminants in closed agricultural systems remain significantly under-investigated (Ediagbonya *et al* 2025, Zhang *et al* 2025). The critical research gap lies in the intersection of microclimate-driven pollutant accumulation and the resulting occupational exposure. Greenhouse environments are characterized by elevated temperatures, limited UV transmittance, and restricted ventilation (Zaimoglu and Baytorun 2018), factors that fundamentally alter the degradation, volatilization, and partitioning of POPs compared to open-field soils. Furthermore, these enclosed systems require intensive manual labor, which can drastically exacerbate human exposure to soil-bound pollutants (Yang *et al* 2014, Ediagbonya *et al* 2025). Consequently, integrating advanced source apportionment (PMF) with a comprehensive, multi-pathway risk assessment (incidental ingestion, dermal contact, and inhalation) is not merely an environmental exercise, but a critical necessity for safeguarding occupational health in intensive farming environments.

To ensure full transparency regarding the dataset, it is explicitly declared that the raw PAH concentration data utilized in this study were previously published as part of a preliminary regional screening

(Olgun and Doğan 2020). However, that earlier work was strictly limited to basic concentration reporting and simple diagnostic ratios. The present manuscript builds upon this foundational dataset to deliver a novel, integrated toxicological and source-apportionment framework. Specifically, the entirely new and previously unpublished contributions of this research include: (1) the analytical quantification of 12 PCB congeners from the greenhouse soils; (2) the application of PMF to robustly and quantitatively apportion the specific emission sources for both PAHs and PCBs; and (3) a comprehensive, multi-pathway (ingestion, dermal, and inhalation) deterministic human health risk assessment specifically tailored for the occupational realities of greenhouse workers.

PMF was applied to soil samples collected from greenhouse farms in Aksu, Antalya, to accurately identify and quantify the specific pollution sources affecting these soils. Furthermore, by employing the United States Environmental Protection Agency (USEPA) deterministic risk models, this research evaluates the incremental lifetime cancer risk (ILCR) of PAHs and the non-carcinogenic Hazard Index (HI) of PCBs for adult greenhouse workers. The objective of this study was to quantify the contributions of various sources to PAH and PCB concentrations in greenhouse soils in the Aksu district of Antalya, Turkiye, using *EPA PMF 5.0*. The aim was to identify the major pollution sources, apportion their relative contributions, provide a detailed understanding of the pathways by which these POPs accumulate in the soil, and examine the effects of covering material (glass or plastic) on sources and source strengths. The results of this analysis offer valuable insights into the environmental impact of greenhouse farming and the potential health risks associated with long-term exposure to these pollutants. These findings also support the development of targeted strategies to mitigate pollution in agricultural soils. Ultimately, this study aims to provide a dual perspective by identifying the major emission sources through PMF and evaluating the overall health status of the greenhouse environment through a quantitative risk assessment.

2. Materials and methods

2.1. Sampling location and sampling points

Antalya is situated on the Turkish Mediterranean coast and had a population of 2.36 million in 2017 . The main sources of income were tourism and agriculture. The region cultivates crops at different elevations, and greenhouse cultivation is prevalent in coastal areas. In Antalya alone, greenhouse cultivation covers approximately 278 million m^2 and produces 3.2 million tons of vegetables annually (Perendeci *et al* 2018)

This study focused on defining the sources of PAHs and PCBs in soil samples from greenhouses in the northwestern part of Fettahlı village, Aksu, Antalya. Farmers in the area cultivate greenhouses once or twice a year based on market demand. If the farmer decides to cultivate twice, the first cycle is in September and the second is in February. If only one cycle was chosen, it was conducted in October after the preliminary work. To eliminate the effect of cultivation time, two sampling campaigns were conducted in September 2017 and February 2018. The average monthly temperatures during these campaigns, as recorded by the Turkish State Meteorological Service, were 25 °C and 11 °C, respectively.

The Aksu-Fettahlı region essentially functions as a closed agricultural micro-basin. Therefore, specific sample selection criteria were established for the study area to maximize comparability: greenhouses utilizing the same groundwater resources and exhibiting uniform soil structures were selected, and sampling was strictly limited to active tomato cultivation. By keeping these fundamental agricultural variables constant, the study aimed to accurately isolate and investigate the specific variations driven by seasonal changes, localized emission sources, and structural cover types (glass versus polyethylene plastic).

Tomatoes account for approximately 50% of the vegetables produced (TUIK 2026). Thus, soil samples were taken from tomato-cultivated greenhouses in both campaigns to assess the effects of seasonal atmospheric emissions and production on the same vegetable. A total of 50 greenhouses and five reference points were sampled during each campaign. Reference points were selected from locations around greenhouses that did not have direct contact with emissions from greenhouse activities and waste. Samples were taken from glass- and polyethylene-covered greenhouses to determine the effect of the greenhouse cover type. Sampling was conducted in an area of approximately 5.83 km^2. The town is located on the Antalya-Isparta intercity highway, and the Antalya International Airport, which receives over 15 million tourists annually, is just 5 km south. Fettahlı is on its flight path, and the region uses wood and coal for household and greenhouse heating, making the area susceptible to various sources of pollution.

In this study, 50 soil samples were collected from 50 greenhouses made of glass or plastic, and five reference samples were collected at reference points during two campaigns: one in the autumn and one

Table 1. Number of samples evaluated in each campaign period.

Cover type	PAH-autumn	PAH-winter	PCB-autumn	PCB-winter
Glass	19	23	22	26
Plastic	23	22	23	22
Reference	3	5	2	5
Total	45	50	47	53

in the winter. The number of samples that passed the quality control (QC) and were evaluated within the scope of this study is shown in table 1.

2.2. Sample extraction, clean-up, and instrumental analysis

2.2.1. Extraction and clean-up procedure

A unified extraction and clean-up protocol was employed for both PAHs and PCBs to maintain analytical consistency. Briefly, 5 g of sieved soil (2 mm) was spiked with target-specific surrogate standards: deuterated PAHs (Acenaphthene-d10, Chrysene-d12, Pyrene-d12, Phenanthrene-d10) for the PAH fraction, and specific PCB congeners (PCB14, PCB65, PCB168) for the PCB fraction. The samples were extracted using 30 ml of an acetone: hexane (1:1) mixture. Following a 24 h dark incubation at room temperature, the samples were subjected to an ultrasonic bath treatment at 15 °C for 60 min. The extracts were additionally centrifuged at 3000 rpm for 15 min to ensure phase separation. The supernatant volumes were reduced to 5 ml using a rotary evaporator and further to 1 ml under a gentle nitrogen stream.

For purification, the extracts were passed through an Agilent Bond Elut SI cartridge (containing Florisil, silica, and alumina). For PAHs, elution was performed with a 20 ml mixture of hexane and acetone (1:1). For PCBs, a sequential elution was applied using 20 ml of hexane followed by 20 ml of acetone. All final fractions were concentrated to 1 ml in hexane under a nitrogen stream prior to chromatographic analysis.

2.2.2. Instrumental analysis and QC

The PAH samples were analyzed using an Agilent 7890/5975 GC MS system. The oven temperature started at 50 °C (1 min), increased to 200 °C at 25 °C min^{-1}, and then to 310 °C at 8 °C min^{-1} (held for 12 min). A 4-point internal calibration (1, 25, 50, and 100 ng ml^{-1}) was utilized ($R^2 > 0.99$).

PCB analysis was performed using an Agilent 7890/5975 GC MS system equipped with an HP5-MS column (30 m × 0.25 mm i.d., 0.25 μm). The oven temperature was programmed to start at 80 °C (held for 2 min), increased to 300 °C at a rate of 30 °C min^{-1}, and finally raised to 320 °C at 10 °C min^{-1} (held for 10 min). A 3-point calibration curve (1, 10, and 50 ng ml^{-1}) was established using a 15-compound PCB mix standard ($R^2 > 0.992$). Target PCBs were explicitly quantified using their specific retention times and the following primary/secondary quantitation ions (m/z): 256/186 for Tri-CBs; 292/220 for Tetra-CBs; 326/254 for Penta-CBs; 360/290 for Hexa-CBs; and 394/296 for Hepta-CBs.

Quality assurance and QC (QA/QC) protocols were implemented for both pollutant classes prior to data analysis. First, the recovery percentiles of the surrogate standards were evaluated. For the PAH fraction, four deuterated standards (Acenaphthene-d10, Chrysene-d12, Pyrene-d12, Phenanthrene-d10) were monitored, and samples with recoveries outside the ±25% range were excluded from the dataset. For the PCB fraction, the recovery efficiencies of the surrogate standards (PCB14, PCB65, PCB168) were 88.8%, 81.4%, and 76.0%, respectively. To monitor potential background contamination, laboratory procedural blanks (using sodium sulfate) were processed alongside the environmental samples, and the final concentrations were blank-corrected. Finally, binary correlations between individual compounds were calculated. Plots were created for correlations with Pearson coefficients above 0.8. A linear trend line and the corresponding 95% confidence interval were drawn, and data points outside this confidence interval were re-examined.

2.3. Source apportionment with PMF

In this study, a PMF model was employed to quantify the source contributions of PAHs and PCBs in soil samples collected from greenhouse farms in Antalya. The analysis was performed using EPA PMF version 5.0, a widely utilized receptor model developed by the U.S EPA. PMF is a multivariate factor analysis method that decomposes the observed pollutant concentrations into two key matrices: source contributions (G) and source profiles (F) (Paatero and Tapper 1994). These matrices collectively provide

a comprehensive understanding of the origin of pollutants and their quantitative impact on environmental samples.

Unlike traditional factor analysis methods, the PMF assigns uncertainty values (u_{ij}) to each data point in the matrix, enabling more robust and reliable source apportionment. The objective function Q is minimized based on the uncertainty values, ensuring that the model optimally fits the observed data while accounting for variability and potential errors associated with each measurement (Norris *et al* 2014). This feature enhances the PMF model's precision in identifying contamination sources in complex environmental datasets, making it a preferred choice in pollution studies (Belis *et al* 2019).

In this analysis, the uncertainty values for each data point were calculated by combining measurement uncertainties and method detection limits (MDLs). The specific MDL values and the detection frequencies (proportion of samples above the detection limit) for all individual PAH and PCB compounds are comprehensively detailed in table S1 (supplementary material). For concentrations below the MDL, a value of half the MDL was used; for missing data, median concentrations were applied, with their corresponding uncertainties set to 4 times the median, following established EPA guidelines (Reff *et al* 2007, Hopke 2016). This approach ensures that missing or censored data does not unduly influence the source apportionment results and that the overall dataset remains consistent and interpretable.

The PMF model decomposes the input concentration matrix X into a product of the source contribution and source profile matrices as follows (equation (1)):

$$X = G\,x\,F + E \tag{1}$$

where G represents the source contribution matrix, F the source profile matrix, and E the residual matrix (Paatero and Tapper 1994). The residuals indicate the difference between the measured concentrations and the modeled values, providing insights into the accuracy of the model. The iterative process aims to minimize the objective function Q, which is defined as (equation (2));

$$Q = \sum_{i=1}^{n}\sum_{j=1}^{m} {e_{ij}}/{u_{ij}} \tag{2}$$

where e_{ij} is the residual, and u_{ij} is the uncertainty associated with each measurement. By minimizing this function, the model ensures that the fit between observed and predicted concentrations is optimized, accounting for data variability.

PMF has been extensively applied in environmental studies, particularly for apportioning sources of PAHs and PCBs in soil, air, and water (Chai *et al* 2017, Ciarkowska *et al* 2022). Its application in this study provides a robust framework for identifying the relative contributions of different sources of these POPs in greenhouse soils, thereby facilitating targeted mitigation strategies.

2.4. Human health risk assessment

To quantify the potential health hazards posed by soil-bound PAHs and PCBs to greenhouse workers, an ILCR and non-carcinogenic HI assessment was performed following the USEPA Risk Assessment Guidance for Superfund (EPA 1989) Greenhouse environments involve intensive manual labor and limited ventilation, creating a unique occupational exposure profile (Nisbet and LaGoy 1992, Emoyan *et al* 2022).

For PAHs, carcinogenic potency was evaluated using the toxic equivalency (TEQ) approach. Measured concentrations were converted into Benzo(a)pyrene equivalents (BaP_{eq}) using toxic equivalency factors (TEFs) (Nisbet and LaGoy 1992). The specific TEF values applied to the individual 16 PAH compounds are explicitly listed in table S2 (supplementary material). To ensure mathematical rigor and capture the exact spatial variability of the sample matrix, the BaP_{eq} concentrations and subsequent ILCR values were calculated for each individual soil sample independently first. These sample-specific values were then averaged across the monitoring network to present the final mean risk.

For PCBs, the dioxin-like congener (PCB 118) was assessed using WHO-2005 TEF values (Van den Berg *et al* 2006) to calculate the toxic equivalent concentration ($C_{soil\,(TEQ)}$, mg kg^{-1}) for the PCB fraction as follows (equation (3))

$$C_{soil\,(TEQ)} = C_{PCB118} \times TEF_{PCB118} \tag{3}$$

where C_{PCB118} is the measured soil concentration of PCB 118 (mg kg^{-1}) and TEF_{PCB118} is the standardized TEF (0.00003). This calculated $C_{soil(TEQ)}$ was subsequently integrated into equations (4)–(6) to determine the pathway-specific chronic daily intakes (CDI_{ing}, CDI_{derm}, and CDI_{inh}) for carcinogenic

risk characterization. The cumulative ILCR for PCB 118 ($ILCR_{PCB118}$) was then quantified using the standard cancer slope factor (CSF) of 1.5×10^5 (mg kg^{-1} $d)^{-1}$ for dioxin-like toxic equivalents, while non-carcinogenic risks for total PCBs were modeled after the toxicological profile of Aroclor 1254 (U.S. EPA 2011).

Chronic Daily Intake (CDI, mg kg^{-1} d) via incidental ingestion (CDI_{ing}), dermal contact (CDI_{derm}), and inhalation (CDI_{inh}) were calculated as follows (equations (4)–(6)):

$$CDI_{ing} = \frac{\left(C_{soil} x\ IngR\ x\ EF\ x\ ED\ x10^{-6}\right)}{(BW\ x\ AT)} \tag{4}$$

$$CDI_{derm} = \frac{\left(C_{soil} x\ SA\ x\ AF\ x\ ABS\ x\ EF\ x\ ED\ x10^{-6}\right)}{(BW\ x\ AT)} \tag{5}$$

$$CDI_{inh} = \frac{\left(C_{soil} x\ InhR\ x\ EF\ x\ ED\ x10^{-6}\right)}{(PEF\ x\ BW\ x\ AT)} \tag{6}$$

where C_{soil} is the equivalent concentration (BaP_{eq}) for PAHs or the total concentration for PCBs (mg kg^{-1}), occupational exposure parameters for adult workers were: IngR = 100 mg day^{-1}, EF = 250 d yr^{-1}, exposure duration (ED) = 25 years, BW = 70 kg, AT = 25 550 d (cancer) or ED × 365 (non-cancer), surface area (SA) = 3 300 cm^2 d^{-1} , adherence factor (AF) = 0.2 mg cm^{-2}, and ABS (absorption) = 0.13 for PAHs and 0.14 for PCBs (U.S. EPA 2011, Ediagbonya *et al* 2025). Inhalation specific pathways were calculated using a standardized inhalation rate (InhR) of 20 m^3 d^{-1} and coupled with a particulate emission factor of 1.36×10^9 m^3 kg^{-1}, both obtained from the U.S. EPA Exposure Factors Handbook (U.S. EPA 2011).

To estimate the carcinogenic risk of PAHs, the ILCR was calculated by multiplying the respective CDI by the CSFs (equation (7)):

$$ILCR = CDI\ x\ CSF \tag{7}$$

where the CSF values were 7.3, 25, and 3.85 (mg kg d^{-1}) for ingestion, dermal contact, and inhalation, respectively, the total ILCR is the sum of risks from all three pathways.

To address the limitations of single-point deterministic calculations and to evaluate parameter uncertainty, a sensitivity analysis incorporating a Monte Carlo simulation (10 000 iterations) was conducted. Key exposure parameters (ED, EF, SA, AF, ABS, and CSFs) were assigned probability distributions. Spearman rank correlation coefficients were calculated to determine the relative influence of each parameter on the variance of the total ILCR.

For the non-carcinogenic risk of PCBs, the hazard quotient (HQ) for each exposure pathway and the overall HI were calculated using the reference dose (RfD) (equations (8) and (9)):

$$HQ = \frac{CDI}{RfD} \tag{8}$$

$$HI = \sum HQ \tag{9}$$

where the RfD for total PCBs is 2.0×10^{-5} mg kg^{-1} day for both ingestion and dermal pathways. According to the U.S. EPA framework, an ILCR $<1.0 \times 10^{-6}$ indicates a negligible risk, values within the range of 1.0×10^{-6}–1.0×10^{-4} represent an acceptable regulatory target, and values exceeding 1.0×10^{-4} or an HI >1.0 denote an unacceptable threat to human health.

3. Results and discussion

3.1. PAH and PCB concentrations in soils

The results of the PAH and PCB analyses are shown in tables 2 and 3, respectively. Autumn and winter season PAH results are shown in the supplementary material tables S3 and S4. The total concentrations of the 16 target PAHs (∑16PAH) in the greenhouse soils ranged from 2.13 to 473.06 ng g^{-1}, with a mean value of 63.72 ng g^{-1}. Similarly, the total concentrations of the 12 PCBs (∑12PCB) ranged from 1.29 to 81.87 ng g^{-1}, with a mean value of 9.70 ng g^{-1}.

The mean PCB concentrations obtained in this study were naturally higher than those reported for remote, pristine background sites, such as the Tibetan Plateau, China (Wang *et al* 2009,

Table 2. Descriptive statistics of PAH concentrations (ng g^{-1}).

Ring number	Compound	Arithmetic mean	Median	Maximum	Minimum	*N*
2-ring	Naphthalene	1.18 ± 0.96	0.96	5.33	0.02	76
3-ring	Acenaphthylene	0.67 ± 0.66	0.50	2.55	0.01	73
	Acenaphthene	1.54 ± 1.4	0.81	4.94	0.27	23
	Fluorene	0.73 ± 0.69	0.50	4.75	0.10	84
	Phenanthrene	7.82 ± 11.11	3.22	61.16	0.01	85
	Anthracene	1.08 ± 1.71	0.46	9.63	0.02	86
4-ring	Fluoranthene	10.33 ± 14.4	4.57	64.89	0.14	87
	Pyrene	8.08 ± 12.27	2.98	57.40	0.04	87
	Benzo(a)anthracene	5.82 ± 10.63	1.71	68.61	0.01	87
	Chrysene	7.75 ± 12.9	3.00	80.54	0.02	85
5-ring	Benzo(b)fluoranthene	7 ± 12.28	2.63	73.96	0.05	86
	Benzo(k)fluoranthene	1.55 ± 2.49	0.58	12.73	0.01	85
	Benzo(a)pyrene	3.23 ± 4.8	1.30	28.72	0.01	87
	Dibenz(a,h)anthracene	1.29 ± 2.16	0.46	12.96	0.01	85
6-ring	Indeno(1,2,3-cd)pyrene	3.47 ± 5.6	1.44	32.37	0.03	87
	Benzo(g,h,i)perylene	4.1 ± 6	1.80	33.16	0.06	87

Table 3. Descriptive statistics of PCB concentrations (ng g^{-1}).

Homolog	Compound	Mean	Minimum	Maximum	Median	*N*
Tri-CB	PCB18	0.76 ± 2.35	0.03	12.19	0.23	26
	PCB20	1.14 ± 1.83	0.03	10.07	0.50	90
	PCB31 + 28	0.18 ± 0.06	0.08	0.25	0.19	8
Tetra-CB	PCB44	2.38 ± 2.87	0.35	5.66	1.13	3
	PCB52	0.99 ± 0.13	0.89	1.08	0.99	2
Penta-CB	PCB101	1.19 ± 1.70	0.06	11.02	0.59	90
	PCB118	1.14 ± 0.83	0.09	5.44	0.98	90
Hekza-CB	PCB138	1.71 ± 2.01	0.12	15.18	1.11	93
	PCB149	1.27 ± 1.85	0.14	13.88	0.67	93
	PCB153	1.25 ± 2.08	0.11	16.54	0.63	92
Hepta-CB	PCB170	0.83 ± 1.03	0.11	7.40	0.58	87
	PCB180	1.07 ± 1.59	0.17	10.99	0.59	90

Zheng *et al* 2012) and pastoral areas in Siberia (Mamontova *et al* 2007). However, as presented in the comprehensive literature comparison (supplementary material table S5), the total PCB levels in Aksu-Fettahlı greenhouse soils remain significantly lower than those found in heavily industrialized or densely populated urban regions globally, such as urban China (Wu *et al* 2011) and London (Vane *et al* 2014), as well as heavily industrialized zones within Turkiye, such as Kocaeli (Cetin 2016).

To empirically validate the premise that greenhouse microclimates act as accumulation sinks for POPs, the contaminant loads in the greenhouse soils were comparatively evaluated against adjacent external reference sites. Due to the limited number of reference samples ($n = 8$ across both campaigns), non-parametric Mann–Whitney U testing did not yield statistically significant differences ($p > 0.05$) for total absolute concentrations. However, explicit enrichment factors clearly demonstrated a net accumulation inside the greenhouses. The mean total PAH concentration in greenhouse soils (63.72 ng g^{-1}) was notably higher than the external background (44.57 ng g^{-1}), yielding internal-to-external enrichment ratios ranging between 1.14 and 2.85 across various congeners. Similarly, the mean total PCB concentration within greenhouses (9.70 ng g^{-1}) surpassed the reference soil baseline (7.50 ng g^{-1}). With the specific exception of PCB 20, almost all targeted PCB congeners exhibited systematically higher accumulation indoors. The higher levels of PCB 20 found in the reference soils are consistent with its established role as an indicator of vehicular exhaust and traffic emissions in the literature (Biterna and Voutsa 2005, Salihoglu *et al* 2011), thereby capturing the direct external influence of the nearby highway. The empirical enrichment of the remaining congeners confirms that the structural enclosure of greenhouses traps both externally deposited atmospheric pollutants and internal agricultural emissions, functioning as a definitive sink for POPs. Furthermore, the limited reference sites were intentionally retained within the PMF receptor model to verify the extent to which the background environment is affected by external pollution sources versus localized greenhouse activities, enabling the model to accurately differentiate the regional baseline from internal agricultural profiles.

To evaluate seasonal variations in pollutant concentrations, distinct statistical methodologies were applied based on the distribution characteristics of the datasets. For PCBs, non-parametric Kruskal–Wallis tests were employed due to severe skewness and the presence of near-detection-limit values. Conversely, for PAHs, a One-Way ANOVA was utilized, leveraging the large sample size ($n = 87$) and the Central Limit Theorem for greater statistical power. The ANOVA results indicated that winter concentrations were statistically significantly higher than autumn concentrations for six low- to medium-molecular-weight PAHs: acenaphthylene ($p = 0.0001$, $F = 16.48$), fluorene ($p < 0.0001$, $F = 19.05$), phenanthrene ($p = 0.0002$, $F = 14.84$), anthracene ($p = 0.0385$, $F = 4.41$), fluoranthene ($p = 0.0130$, $F = 6.42$), and pyrene ($p = 0.0284$, $F = 4.96$). The lack of significant seasonal variation ($p > 0.05$) for the heavier, 5- and 6-ring PAHs suggests that these high-molecular-weight compounds are more persistent and tightly bound to the soil matrix, resisting short-term seasonal meteorological fluctuations.

The significant enrichment of these six specific low- to medium-molecular-weight PAHs during the winter campaign can likely be attributed to a combination of their physicochemical properties and seasonal agricultural practices. Primarily, these 3- and 4-ring congeners possess relatively higher volatility compared to heavier PAHs; thus, diminished ambient temperatures in winter are thought to reduce their volatilization, promoting stronger partitioning and accumulation within the soil matrix (Bozlaker *et al* 2008). Additionally, these lighter compounds are highly susceptible to UV-driven photodegradation under intense autumn solar radiation, a degradation pathway that is largely mitigated during the winter months (Baek *et al* 1991, Perraudin *et al* 2007). Finally, the onset of intensive winter cultivation cycles often coincides with the increased application of specific crop protection products. For instance, compounds such as phenanthrene and fluoranthene have been associated with certain pesticides and agrochemicals (Abdel-Shafy and Mansour 2016), which may further explain their targeted elevation in the greenhouse soils during the winter campaign.

To evaluate the influence of greenhouse cover materials, statistical and correlational comparisons were performed between glass and polyethylene plastic greenhouses. While statistical tests (ANOVA for PAHs and Kruskal–Wallis for PCBs) of the absolute total concentrations indicated no significant differences ($p > 0.05$) overall, largely due to high spatial variability across the sites, the inter-compound correlation matrices revealed distinct microclimate dynamics.

For PAHs, the physical differences between covers are thought to manifest primarily through UV-driven photodegradation. Glass greenhouses generally allow higher UV transmittance compared to UV-blocking agricultural plastics. In the literature that the half-lives of PAHs are significantly reduced under solar radiation and ozone exposure due to rapid photodegradation (Baek *et al* 1991, Perraudin *et al* 2007). As a result, during the high-sunlight autumn campaign, specific PAH congeners in glass greenhouses likely experienced selective photodegradation, which is believed to have decoupled their co-accumulation (supplementary table S6). Correlation analysis demonstrated this effect clearly: Phenanthrene and Chrysene were significantly correlated under plastic covers ($r = 0.695$, $p < 0.01$) but showed no significant correlation under glass ($r = 0.396$, $p > 0.05$). Similarly, pyrene and Benzo(a)anthracene exhibited a near-perfect coupling in plastic greenhouses ($r = 0.919$, $p < 0.01$) that was notably weakened in glass environments ($r = 0.692$, $p < 0.01$). Conversely, during the winter campaign, when solar radiation and UV intensity were naturally diminished, this photodegradation effect appeared to be mitigated. Consequently, the inter-compound correlations in glass greenhouses were restored to highly significant levels (e.g. $r = 0.888$, $p < 0.01$ for Phenanthrene and Chrysene), closely mirroring the robust accumulation patterns observed in the plastic environments (supplementary table S7).

For PCBs, the dynamics were likely primarily governed by ventilation practices. Previous studies have highlighted that meteorological factors, including wind and air circulation, critically control the partitioning, volatilization, and spatial homogenization of PCBs in soils (Meijer *et al* 2003, Wu *et al* 2011). Plastic greenhouses, characterized by intense side and roof ventilation, promote rapid air circulation and a more homogeneous mixing of atmospherically deposited pollutants compared to the more stagnant microclimate of glass environments. Consequently, specific PCB congeners in plastic greenhouses exhibited significantly stronger inter-compound associations. During the autumn campaign (supplementary table S8), the correlation between PCB 138 and PCB 101 was remarkably robust under plastic ($r = 0.792$, $p < 0.01$), whereas it was notably weaker under glass ($r = 0.442$, $p < 0.05$). This phenomenon persisted during the winter campaign (supplementary table S9), where heavy congeners like PCB 138 and PCB 180 showed highly significant coupling in plastic greenhouses ($r = 0.877$, $p < 0.01$) but only moderate association under glass ($r = 0.561$, $p < 0.01$). Ultimately, while absolute mass accumulation differences were moderate, the environmental behavior, co-accumulation, and degradation patterns of POPs appear to be fundamentally driven by the UV transmittance and ventilation properties of the cover types.

3.2. Sources of PAHs

The EPA PMF 5.0 program was used to identify the active PAH sources in the region and their contribution ratios. Solutions between 3 and 6 factors were examined. In all solutions, source profiles, relationships between modeled and observed PAH concentrations, and relationships between source contributions (*G*-scores) were evaluated. Acenaphthylene was excluded from the dataset due to a large amount of data (>90%) being below the detection limit, and naphthalene was excluded due to the low relationship between modeled and observed concentrations. Similarly, three points with low modeling performance and increased *Q* values (27 Winter, 3 Summer, and 17 Summer) were also excluded from the dataset. As a result, PMF was run on 14 compounds and 92 soil samples (84 greenhouse and eight references), and five sources were identified as active in the region. To assess the stability of the solution and rotational ambiguity, standard error diagnostics (BS, DISP, and BS-DISP) were applied. The initial unrotated base run exhibited notable rotational ambiguity during BS-DISP resampling (with an 18% acceptance rate and significant factor swapping). This provided the empirical justification for applying a rotational parameter (F_{peak}) of −0.5. By setting F_{peak} to −0.5, we effectively minimized the rotational ambiguity between closely related combustion sources without significantly increasing the *Q* value. The stability of this finalized, rotated model is confidently supported by the DISP results, which showed minimal swapping (only 2 swaps across the 5 factors: 0, 0, 1, 1, 0), and high Bootstrap (BS) mapping scores (matching 95%, 98%, 87%, 90%, and 99% of the resampling runs using a correlation threshold of $R > 0.6$). Furthermore, quantitative diagnostics indicated an excellent model fit: the Q_{robust}/Q_{true} ratio was 0.998 (981.1/983.3), ensuring that peak events did not disproportionately dominate the solution, and the $Q_{true}/Q_{expected}$ ratio was 1.30 (983.3/758). The scaled residuals were symmetrically distributed, with approximately 99.1% of the data points falling within the widely accepted limits of −3.0 to +3.0. The mass distribution of the five sources obtained is shown in figure 1. It was observed that a significant portion of the PAHs in the region's soil was attributable to diesel engine combustion (33%). However, while the effects of greenhouse emissions (pesticide use, greenhouse plastics, and paint) and coal combustion emissions were observed to be around 21%, emissions from gasoline vehicles accounted for 20% of the modeled PAHs. As the sampling area is located on the flight path of aircraft landing and taking off from Antalya Airport, jet fuel used by aircraft was determined to account for 5% of the modeled PAH mass. Seasonal variations in the contributions of sources are presented in table 4. The contributions of all factors were higher in winter than in summer. The only statistically significant difference between the averages of source contributions was observed in the mixed greenhouse source factor.

The source profile for the first factor and the explained mass percentages of PAHs are shown in figure 2(a). In this factor, 40% to 60% of the 5- and 6-ring PAHs are accounted for. Additionally, 10% to 20% of the mass of BaA, Chr, Anp, and Flr is accounted for by this factor. In the literature, DahA, IcdP, and BgihPy are reported to be indicators of motor vehicle emissions (Cetin 2016). However, it has also been frequently noted that BkF, BbF, Chr, and BaA are observed in emissions from motor vehicles using fossil fuels (Khalili *et al* 1995, Ravindra *et al* 2008, Simcik *et al* 1999; S. Wang *et al* 2013). However, BaP is generally emitted from gasoline-powered vehicles (Devi *et al* 2016). Furthermore, Py and Chr are expected to be observed at higher levels in diesel vehicles. Therefore, this factor is thought to be due to PAHs emitted by gasoline-powered vehicles. This factor accounts for 12.05 ng g^{-1} of the modeled PAH. The distribution of the source in greenhouses for the autumn and winter months is shown in the supplementary material, figures S1 and S2, respectively. A more intense contribution was observed in greenhouses on the western side during both the autumn and winter periods. The high contribution in greenhouses west of the Antalya-Isparta highway is thought to be due to wind transport.

The source profile of the second factor is shown in figure 2(b). Approximately 45% of the An mass is explained by this factor. In addition to An, the factor profile also includes Phe, Flu, Py, BaA, and Chr. In a study conducted in Rome, 23 PAH compounds were identified at three different points of the airport. According to the study, measurements on the apron showed the highest PAH levels, led by 2- and 3-ring PAHs, and it was concluded that methylnaphthalene and acenaphthene (An) could be associated with jet fuel emissions (Cavallo *et al* 2006). Similarly, in Los Angeles, values measured downwind of the aircraft takeoff runway were compared with background values, and PAHs from Phe to Chr were found to exceed background levels (Zhu *et al* 2011). Antalya Airport is located approximately 8 km from the sampling area. The map showing the sampling area on the noise map prepared by TUBITAK is shown in supplementary material figure S3. Although we do not expect noise to correlate with the behavior of gases and particles in the atmosphere, the noise map provides information about aircraft routes.

The sampling area, Fettahlı, is located under the flight paths. Therefore, in this study, it is thought that the profile observed in Factor 2 is caused by the combustion of fuel from aircraft landing and

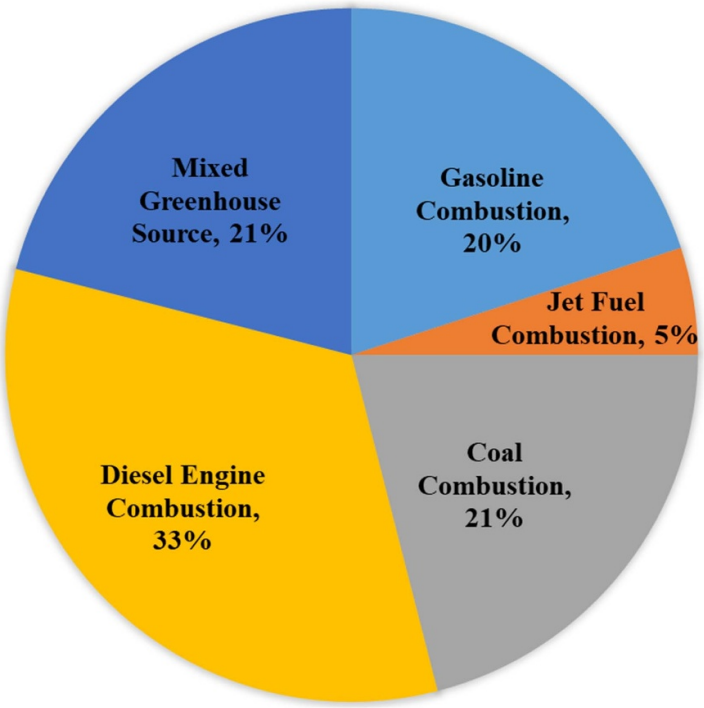


Figure 1. Source contribution ratios of modeled PAH sources.

taking off at Antalya Airport. The distribution of this factor in greenhouses for the autumn and winter months is shown in supplementary material figures S4 and S5, respectively. While a more homogeneous distribution is observed in the autumn period, in the winter period, source contributions are more intense in greenhouses located in western regions. This situation is thought to be due to the airport, which has three runways, one of which is military, using only the non-military runway in the west during the winter months.

Figure 2(c) shows the source profile of the third factor and the variance of PAHs explained by the factor. Approximately 30%–40% of Py, BaP, and Flu is explained by the factor. The factor also explains twenty percent of AnP, Phe, An, and BaA. According to the literature, a typical coal combustion profile contains Flu, Py, and AnP (Dumanoglu *et al* 2017). Chr is considered an indicator of coke and biomass combustion. An, Phe, Flu, Py, and Chr are PAHs formed as a result of wood combustion. Therefore, this factor is thought to be formed as a result of coal and wood combustion. Since winter temperatures were high when sampling was carried out, the survey found that the majority of farmers did not use any fuel during that period. Consequently, no significant difference was observed in source contributions between the autumn and winter periods. The seasonal variation in source contributions is shown in supplementary material figures S6 and S7. It was determined that the contribution of greenhouses to this source was not concentrated in a specific area. Although fuel is not used in greenhouse activities, it is thought that residential fuel use by people living in homes in the area also contributes to this factor. This factor accounts for 12.40 ng g^{-1} of the modeled mass.

The source profile of the fourth factor is shown in figure 2(d). In this factor, approximately 50% of BaA, Chr, and BaF, and 40% of BkF, DahA, and IcdP are explained. Flu, Py, and BgihPy are explained at around 30% in the factor. As explained in the first factor, DahA, IcdP, and BghiPy are emitted by motor vehicles. Other motor vehicle indicators, BaA, BaF, and BkF, contribute significantly to this factor. Chr and Py, which are PAHs that distinguish diesel vehicles from gasoline vehicles, are observed in this factor. Therefore, this factor is thought to be PAHs emitted by diesel vehicles. This factor explains 19.70 ng g^{-1} of the modeled mass. The seasonal variation in source contributions is shown in supplementary material figures S8 and S9. When examining the spatial distribution of this factor's contributions, a stronger contribution was observed in greenhouses located in the west. Although this factor originates from vehicles using the Antalya-Isparta road, as with gasoline vehicles, emissions from diesel-fueled vehicles used for greenhouse activities are also thought to contribute to the factor.

The source profile of the last factor is shown in figure 2(e). In this factor, approximately 80% of Flr and approximately 60% of AnP and Phe are explained. Low contributions from Flu, An, and Py

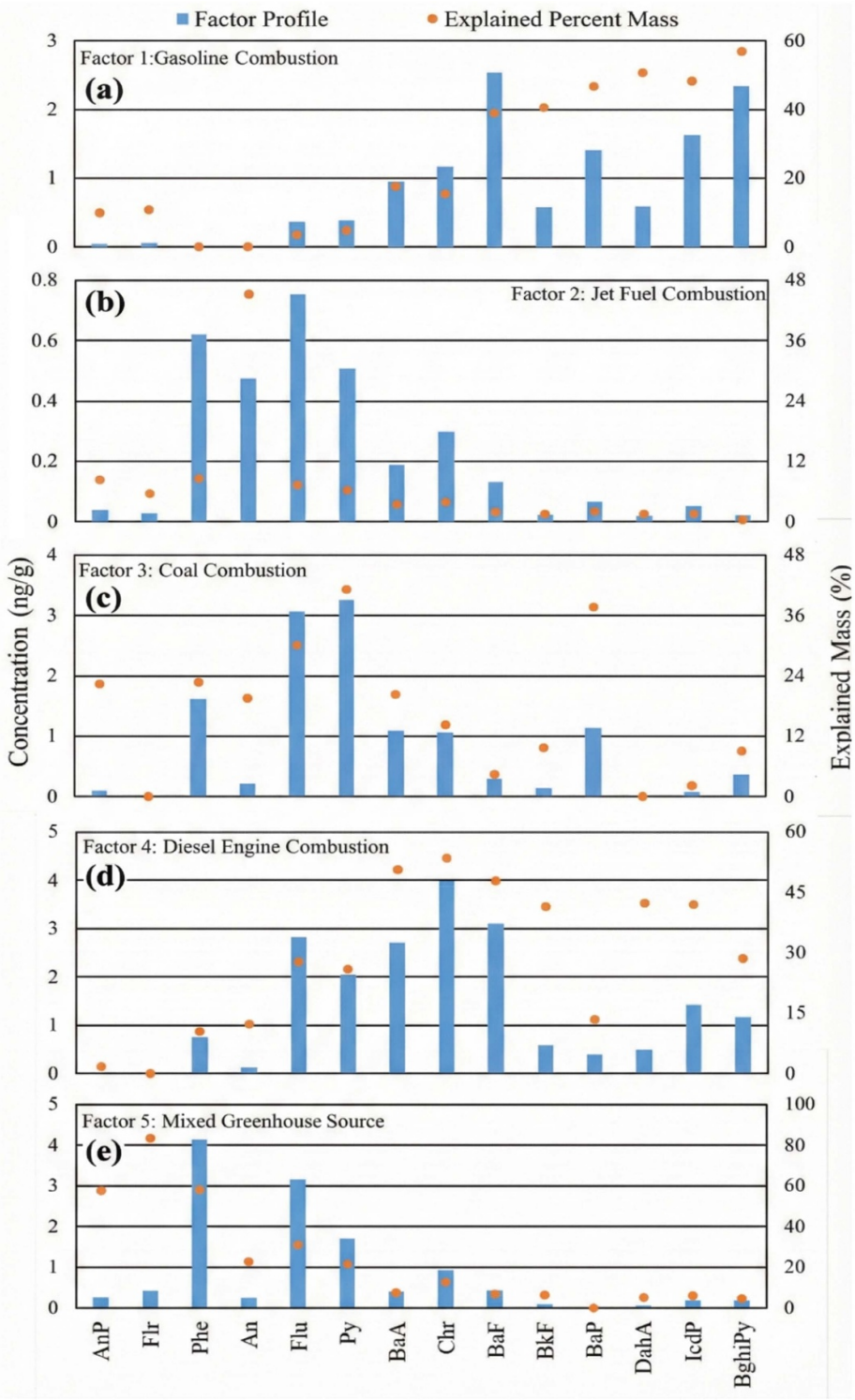


Figure 2. Factor profiles and explained mass percentage of PAHs for (a) Gasoline combustion, (b) Jet fuel combustion, (c) Coal combustion, (d) Diesel engine combustion, and (e) Mixed greenhouse source.

are also observed in the factor. AnP and Flr are used in plastics. AnP, An, Flu, and Flr are used in paints. Furthermore, Phe is used in pesticides, and Flu is used in agrochemicals (Abdel-Shafy and Mansour 2016). Overall, the compounds emitted by these activities (painting greenhouses, using pesticides and agrochemicals in greenhouses, and the presence of plastic components) are included in this factor. Therefore, this factor has been defined as emissions resulting from greenhouse activities. The contribution maps for the autumn and winter sampling are shown in supplementary material figures S10 and S11. In this factor, a statistical difference was observed between the contributions of the seasons (table 4). Several reasons are considered for this difference. The first is that greenhouse activities are

Table 4. Seasonal average values of source contributions (*G*-score).

Sources	Autumn	Winter
Gasoline combustion	0.81	1.02
Jet fuel combustion	0.84	1.03
Coal combustion	0.61	1
Diesel engine combustion	0.72	1.04
Mixed greenhouse sources[a]	0.43	1.01

[a] There is a statistically significant difference between the contributions in autumn and winter months within a 95% confidence interval.

just beginning during the autumn sampling period. Second, greenhouses are ventilated more during the autumn period because the weather is warmer, thus dispersing pollution within the greenhouse before it accumulates. Finally, pollution accumulates within the greenhouse due to greenhouse activities. This factor accounts for 12.30 ng g^{-1} of the modeled mass.

While natural processes inherently contribute a baseline concentration to the soil PAH matrix, the source apportionment in this study exclusively resolved anthropogenic factors. It should be noted that isolating natural profiles in receptor models strictly requires specific chemical tracers, such as biogenic perylene or specific alkylated derivatives. Because this study focused on the 16 US EPA priority PAHs, which primarily serve as indicators for anthropogenic activities, no specific tracer for natural sources could be identified within the modeled dataset. Consequently, the inability to distinctly separate the natural PAH baseline without specialized biomarkers represents an inherent methodological limitation, and the apportioned profiles predominantly reflect anthropogenic inputs rather than natural pedogenic processes.

3.3. Sources of PCBs

PCB sources and their contribution ratios were determined using EPA PMF 5.0. The compounds PCB 18, PCB 31 + 28, PCB 44, and PCB 52 were excluded from the dataset because they accounted for less than 90% of the data. As a result, the EPA PMF 5.0 program was run on a dataset containing eight compounds and 91 sample examples. Results for 2–5 factors were evaluated, and the optimal number was determined to be 3. When determining the number of factors, source profiles, and relationships between modeled and observed PCB concentrations, as well as between source contributions (*G*-scores), were evaluated. The stability of the identified PCB sources was evaluated using PMF error diagnostics. The unrotated base model demonstrated stability natively. The Bootstrap (BS) mapping showed a perfect 100% match (100 out of 100 runs) across all three factors. Furthermore, the DISP analysis resulted in zero factor swaps (0, 0, 0) across the 3-factor solution. Because the unrotated base model was unequivocally stable with negligible rotational ambiguity, no forced rotation (F_{peak}) was mathematically or physically warranted. Quantitative diagnostics further supported the robustness of the solution: the Q_{robust}/ Q_{true} ratio was excellent at 0.978 (841.6/860.7), proving that peak events did not skew the model. The Q_{true}/ $Q_{expected}$ ratio was 1.95 (860.7/441), which is a common and acceptable occurrence in environmental datasets reflecting slightly conservative input uncertainty estimations. Finally, the scaled residuals demonstrated symmetry, with approximately 97.8% of the data points falling within the optimal limits of −3.0 to +3.0.

Figure 3 shows the PCB contribution rates to sources based on the modeling results. The greenhouses sampled are located along the Isparta-Antalya D685 highway, and wood and coal are used for heating. During sampling, open burning was observed near the greenhouses, and it is estimated that waste materials from the greenhouses were burned there for disposal during and after planting preparation.

The factor 3, estimated to be caused by atmospheric transport, burning, commercial PCB mixtures, and other greenhouse and non-greenhouse activities, accounted for the largest share of the analyzed greenhouse soils at 60%. Factor 2, referred to as wood and coal burning for heating purposes, contributed 19%. This is thought to be due to the mild winter during the sampling period and the resulting low use of wood and coal for heating. Factor 1, referred to as used motor oil, waste oil combustion,

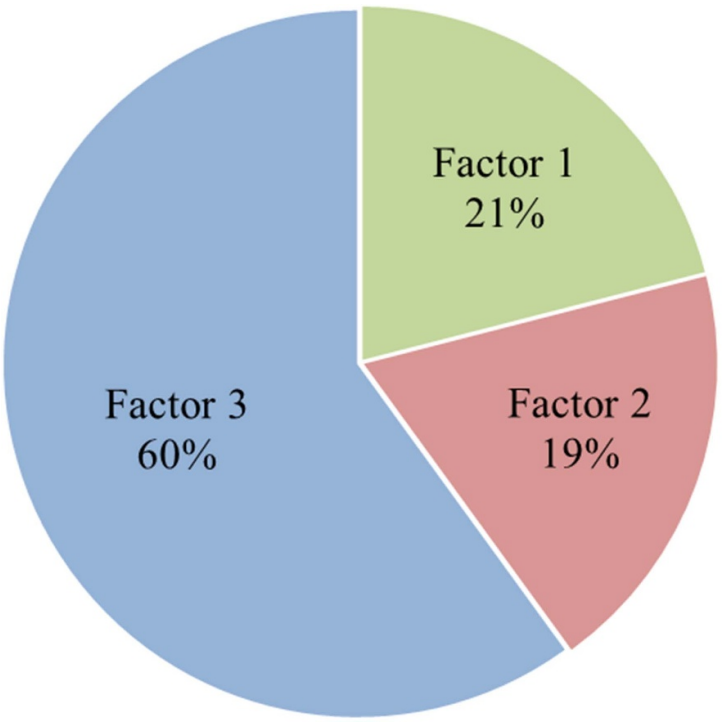


Figure 3. Source contribution ratios of modeled PCBs.

Table 5. Seasonal average values of source contributions (*G*-score).

Sources	Autumn	Winter
Use of used motor oil, waste oil combustion, and vehicle exhaust	0.60	1.34
Burning wood and coal for heating purposes	1.06	0.98
Mixed	1.16	0,89

and vehicle exhaust, contributed 21%. This factor is thought to be due to vehicle use in greenhouses for preparation during the planting season and to atmospheric transport from the highway near the greenhouses. Seasonal variations in the contributions of sources are presented in table 5. There is no statistically significant difference between the averages of source contributions.

The Kruskal–Wallis test was performed to determine whether there were significant differences between the factors, sampling period, and cover type using the *G* scores of the three factors obtained through PMF. When conducting the Kruskal–Wallis test, normality tests were first performed.

When determining normality, skewness and kurtosis values (Skewness and Kurtosis) were used as a basis, and values within the range of −1 and +1 were considered to have a normal distribution. To determine normality, skewness and kurtosis were used, and values within the range of −1 to +1 were considered normally distributed. Across all cover types and seasons, no statistically significant differences were found for any factor. Although not statistically significant, it was determined that winter plastic concentrations in factors 1 and 3 were higher than in the others. Table 6 shows the results of the Kruskal–Wallis test.

The source profile of the first factor is shown in figure 4. This factor is explained as PCB 20 from the tri-CB homolog group, gasoline vehicle emissions, and the burning of waste oils. The literature reports that PCB concentrations are higher in areas with heavy traffic than in areas with light traffic. Vehicle traffic can be a source of PCBs in the atmosphere (Biterna and Voutsa 2005). Furthermore, Brož *et al* (2000) determined that gasoline vehicles contain PCB, that PCB emissions from mineral oils used in vehicle engines depend on vehicle mileage, that vehicles with over 10 000 km cause higher PCB emissions, and that the technical condition of the engine also affects PCB emissions. According to Salihoglu *et al* (2011), low-molecular-weight PCBs, including tri-CBs, originate from traffic. PCB 20 contributed 21% to the total variance and 96.4% to factor 1. Furthermore, PCBs 118 (15.5%) and 138 (11.7%) also contributed to this factor. It is thought that wind transport from the Antalya-Isparta highway, vehicle use within the greenhouse, and burning waste oil near the greenhouse contributed to this factor.

Table 6. Kruskal–Wallis test values.

Factor	Sampling period and cover type	*N*	Rank average	Chi-squared	*p*
Factor 1	Autumn glass	22	50.41	3.60	0.31
	Autumn plastic	23	40.30		
	Winter glass	26	44.04		
	Winter plastic	22	54.09		
Factor 2	Autumn glass	22	45.23	0.44	0.93
	Autumn plastic	23	44.98		
	Winter Glass	26	49.06		
	Winter plastic	22	48.45		
Factor 3	Autumn glass	22	45.45	4.34	0.23
	Autumn plastic	23	41.48		
	Winter glass	26	44.62		
	Winter plastic	22	57.14		

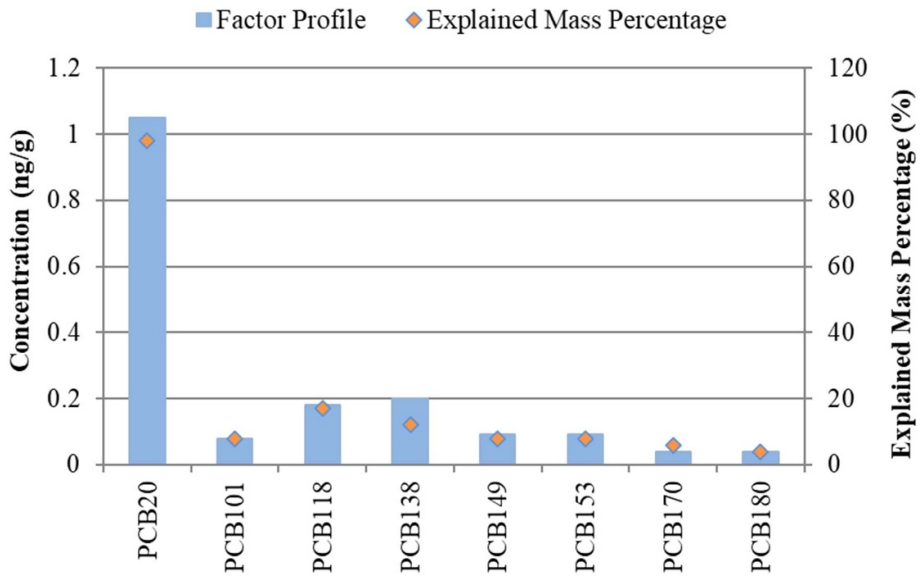


Figure 4. Factor profile and explained mass percentage of PCBs for factor 1.

Figure 5 shows the source profile of the second factor. This factor accounted for 19% of the total variance. This factor includes PCB 118, which is found in the pentaCB homolog group. PCB 118 accounted for 67% of this factor. In addition, PCB 138 (15.3%), PCB 149 (13.4%), PCB 153 (13.9%), PCB 170 (17.9%), and PCB 180 (16.2%) also contributed to this factor. The literature indicates that PCB 118 originates from the incineration of electronic waste (Chakraborty *et al* 2018), medical waste (Chakraborty *et al* 2016), and wood and coal (Aydin *et al* 2014, Dumanoglu *et al* 2017, Cetin *et al* 2018). Lee *et al* (2005) reported that PCB 118 was predominant in coal and hardwood combustion emissions. Furthermore, PCB 118 is the most prevalent congener emitted from coal-fired power plants (Biterna and Voutsa 2005). In the survey conducted for the greenhouses sampled in this study, it was reported that coal and wood were used for heating purposes. This factor is thought to be contributed to by the use of wood and coal for heating in greenhouses and nearby residences, and by waste incineration for disposal.

The source profile of the last factor is shown in figure 6. According to the literature, PCB 101 originates from various combustion processes (Lee *et al* 2005, Chakraborty *et al* 2016, Yurdakul *et al* 2019) and technical PCB mixtures (Dumanoglu *et al* 2017), while PCB 118 is sourced from wood and coal combustion (Lee *et al* 2005, Dumanoglu *et al* 2017), municipal waste incineration (Chakraborty *et al* 2016), and technical PCB mixtures (Dumanoglu *et al* 2017). PCB 138 is reported to originate from biomass combustion (Eckhardt *et al* 2007), atmospheric transport (Kurt-Karakus *et al* 2018), technical PCB mixtures (Odabasi *et al* 2016), and e-waste shredding (Chakraborty *et al* 2018); PCB 153 originates from domestic fuel combustion (Yurdakul *et al* 2019) and atmospheric transport (Kurt-Karakus

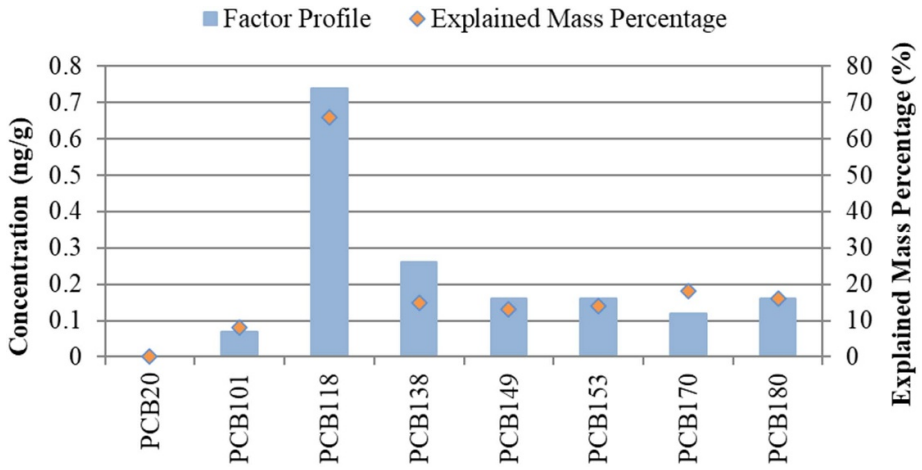


Figure 5. Factor profile and explained mass percentage of PCBs for factor 2.

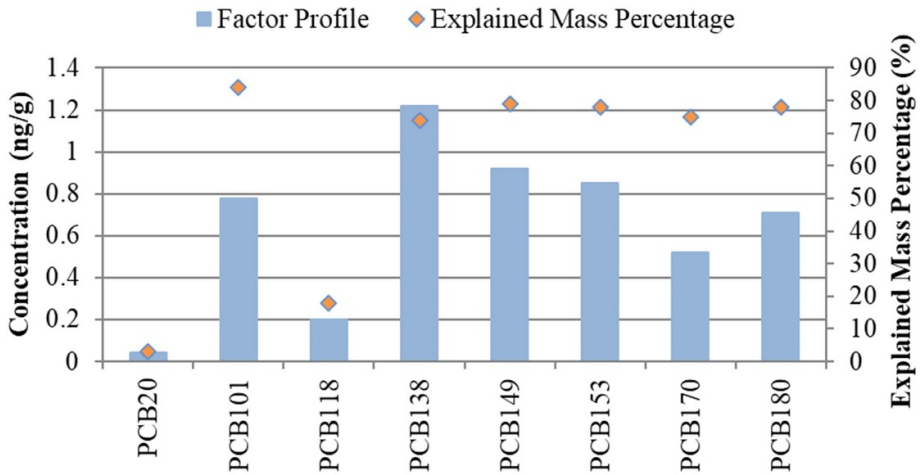


Figure 6. Factor profile and explained mass percentage of PCBs for factor 3.

et al 2018); PCB 170 and PCB 180 originate from technical mixtures (Aydin *et al* 2014, Cetin *et al* 2018). However, since these congeners could not be shown as separate factors in this study, they are referred to as a mixed factor.

3.4. Occupational health risk implications

The integration of chemical profiles with health risk assessment translates the measured concentrations into actionable toxicological insights. The total BaP_{eq} for greenhouse soils was 6.42 ng g^{-1}. The deterministic ILCR assessment yielded a total carcinogenic risk of 6.45×10^{-5} for adult greenhouse workers. This value falls within the acceptable regulatory target range of 1.0×10^{-6}–1.0×10^{-4} established by the U.S. EPA framework, indicating that the carcinogenic risk from PAH exposure is present but remains within the managed safety limits.

In our greenhouse scenario, the deterministic calculations indicated that dermal contact accounted for 74.6% of the total carcinogenic risk. However, it must be acknowledged that this high contribution is primarily a mathematical consequence of the toxicological parameter inputs rather than an independent environmental finding. Specifically, the high dermal CSF (25 (mg kg^{-1} $d)^{-1}$) relative to the ingestion CSF (7.3 (mg kg^{-1} $d)^{-1}$), coupled with the large skin SA and AF multipliers assigned for agricultural labor, inherently amplifies the dermal risk output. To evaluate this, a sensitivity analysis (supplementary material figure S12) was conducted. The Spearman rank correlation revealed that Dermal ABS (ABS, $r = 0.50$), ED (ED, $r = 0.44$), and AF (AF, $r = 0.40$) introduced the greatest variance into the total risk estimations, alongside the dermal CSF ($r = 0.33$). While this parameter-driven dominance is consistent with models applied in other agricultural contexts (Yang *et al* 2014, Ediagbonya *et al* 2025), it fundamentally confirms that the structure of the exposure models governs the cumulative risk outcomes.

Consequently, occupational health interventions in greenhouses should focus heavily on mitigating direct soil-to-skin contact, as the model sensitivity confirms this interface dictates the overall risk.

Regarding PCBs, the calculated HI for non-carcinogenic risk was 1.30×10^{-3}, which is orders of magnitude below the safety limit of 1.0. This negligible toxicological risk aligns with the findings of Emoyan *et al* (2022), who observed that while PCBs persist near emission nodes, they rarely trigger acute non-carcinogenic crises in topsoils unless massive industrial dumping occurs. The non-carcinogenic risk model for PCBs involves specific toxicological uncertainties that require delineation. In this study, the non-carcinogenic hazards of the total measured PCBs were evaluated using the RfD of Aroclor 1254 (2.0×10^{-5} mg kg^{-1} d). Although the PMF receptor model indicates that the localized PCB profile is predominantly driven by atmospheric transport and secondary combustion processes rather than direct technical commercial mixtures, applying the Aroclor 1254 benchmark serves as a conservative screening threshold recommended by the U.S. EPA in the absence of congener-specific non-carcinogenic values. However, this extrapolation introduces systematic uncertainties, as environmental weathering and transport processes alter the congener distribution relative to the original commercial formulations. Furthermore, due to the absence of an official U.S. EPA inhalation reference concentration for total PCBs in the IRIS database, the inhalation HQ (HQinh) was omitted from the cumulative calculations. Consequently, the reported HI strictly represents the combined toxicological stress of the incidental ingestion and dermal contact pathways.

To address the toxicological asymmetry between the contaminant classes, the carcinogenic risk derived from the dioxin-like congener (PCB 118) was formally quantified. The ILCR for PCB 118 (ILCRPCB118) was calculated across the three primary exposure pathways, yielding a cumulative mean value of 5.17×10^{-6}. This value falls within the acceptable regulatory target range (1.0×10^{-6}–1.0×10^{-4}) defined by the U.S. EPA. However, it is crucial to emphasize that this risk originates from only one congener. Because PCB 118 represents the sole dioxin-like compound evaluated among the 12 target PCBs in this study, its standalone risk of 5.17×10^{-6} strictly serves as a lower-bound estimate. Rather than suggesting a low overall PCB risk, this finding highlights that unmeasured dioxin-like PCBs could potentially contribute to a significantly higher cumulative risk profile. Therefore, the true representativeness of the dioxin-like risk characterization remains inherently limited by this analytical constraint, underscoring the necessity for comprehensive DL-PCB monitoring in future greenhouse soil studies.

4. Conclusion

Within the scope of this study, PAH and PCB concentrations were determined in tomato-cultivated greenhouse soils in the Aksu-Fettahlı region of Antalya, a province of significant importance to Turkish greenhouse agriculture. The variation in these concentrations was investigated by season (autumn and winter) and cover type (plastic and glass). A total of 50 greenhouse soil samples (25 plastic, 25 glass) and 5 reference samples were collected.

Concentrations in plastic versus glass greenhouses across different seasons were evaluated and compared with international literature. Compared with the international literature, while the measured concentrations were naturally higher than remote background sites like the Tibetan Plateau, they remained significantly lower than the levels documented in heavily industrialized or densely populated urban regions globally (e.g. urban China, London) and were comparable to moderately affected areas in Turkiye.

Source apportionment using PMF identified five active PAH sources. Diesel engine combustion (33%) was the primary contributor to PAH contamination, followed by mixed greenhouse activities (pesticides, plastics, and paint, 21%), coal combustion (21%), gasoline emissions (20%), and jet fuel emissions (5%). Only the mixed greenhouse source factor showed statistically significant seasonal variation.

For PCBs, three factors were identified. The largest contributor (60%) was a ‘Mixed’ factor dominated by PCB 101, 138, 149, 153, 170, and 180, likely originating from atmospheric transport and commercial PCB mixtures. The second factor (21%) consisted of used motor oil, waste oil combustion, and vehicle exhaust, influenced by wind transport from the Antalya-Isparta highway and by emissions from internal greenhouse activities. The final factor (19%) was attributed to wood and coal combustion for heating. The mild winter during the sampling period led to lower heating emissions, which explains the lack of significant seasonal variation in PCB levels.

Furthermore, integrating these source profiles with human health risk assessment revealed that, while the current ILCR for PAHs and the HI for PCBs remain within toxicologically safe limits, the synergistic accumulation of these pollutants necessitates proactive management. Notably, dermal contact was

identified as the overwhelmingly dominant exposure pathway for greenhouse workers. The study concludes that while specific sources such as diesel combustion and internal greenhouse activities significantly contribute to soil PAH and PCB levels, the overall human health risk remains below priority management thresholds. However, the dominance of the dermal exposure pathway suggests that protective measures for workers should be considered as part of sustainable greenhouse management. Overall, this study serves as a critical baseline for greenhouse soil quality and occupational safety in Antalya. Future research should expand into other Mediterranean regions and incorporate both organic and inorganic pollutant groups to comprehensively minimize POP exposure originating from agricultural and external activities.

Acknowledgments

The authors dedicate this work to the memory of Professor Dr Gürdal Tuncel and Professor Dr Semra Tuncel for their invaluable mentorship and profound contributions to our professional development.

Data availability statement

The data cannot be made publicly available upon publication because no suitable repository exists for hosting data in this field of study. The data that support the findings of this study are available upon reasonable request from the authors.

Supplementary Data available at: https://doi.org/10.1088/2515-7620/ae9680/data1.

Funding

This study was supported by the Research Fund of Akdeniz University, Project Numbers: FYL-2020-5271 and FYL-2018-3645.

Ethics approval

Not applicable. This study did not involve human participants, animals, or any activities requiring ethical approval.

Consent for publication

Not applicable. No identifiable personal data or images of individuals are included in this manuscript.

Conflict of interest

The authors declare that they have no known competing financial interests or personal relationships that could have appeared to influence the work reported in this paper.

Author contributions

Güray Doğan
Conceptualization (equal), Methodology (lead), Project administration (lead), Supervision (lead), Writing – original draft (supporting), Writing – review & editing (supporting)

Ahmet Mustafa Tepe 0000-0002-5210-6291
Conceptualization (equal), Formal analysis (equal), Software (lead), Writing – original draft (equal), Writing – review & editing (lead)

Ebru Nur Dokumacı
Resources (equal), Visualization (equal), Writing – original draft (supporting)

Bihter Olgun
Resources (equal), Visualization (equal), Writing – original draft (supporting)

References

Abdel-Shafy H I and Mansour M S M 2016 A review on polycyclic aromatic hydrocarbons: source, environmental impact, effect on human health and remediation *Egypt. J. Pet.* **25** 107–23

Aydin Y M, Kara M, Dumanoglu Y, Odabasi M and Elbir T 2014 Source apportionment of polycyclic aromatic hydrocarbons (PAHs) and polychlorinated biphenyls (PCBs) in ambient air of an industrial region in Turkey *Atmos. Environ.* **97** 271–85

Baek S O, Goldstone M E, Kirk P W W, Lester J N and Perry R 1991 Phase distribution and particle size dependency of polycyclic aromatic hydrocarbons in the urban atmosphere *Chemosphere* **22** 503–20

Belis C A, Pikridas M, Lucarelli F, Petralia E, Cavalli F, Calzolai G, Berico M and Sciare J 2019 Source apportionment of fine PM by combining high time resolution organic and inorganic chemical composition datasets *Atmos. Environ. X* **3** 100046

Biterna M and Voutsa D 2005 Polychlorinated biphenyls in ambient air of NW Greece and in particulate emissions *Environ. Int.* **31** 671–7

Bozlaker A, Muezzinoglu A and Odabasi M 2008 Atmospheric concentrations, dry deposition and air–soil exchange of polycyclic aromatic hydrocarbons (PAHs) in an industrial region in Turkey *J. Hazard. Mater.* **153** 1093–102

Brož J, Grabic R, Kilián J, Lojkásek M, Marklund S, Ocelka T, Pekárek V, Přibyl J, Tydlitát V and Výška J 2000 The effect of oils on PAH, PCDD, PCDF, and PCB emissions from a spark engine fueled with leaded gasoline *Chemosphere* **41** 1905–11

Cavallo D, Ursini C L, Carelli G, Iavicoli I, Ciervo A, Perniconi B, Rondinone B, Gismondi M and Iavicoli S 2006 Occupational exposure in airport personnel: characterization and evaluation of genotoxic and oxidative effects *Toxicology* **223** 26–35

Cetin B 2016 Investigation of PAHs, PCBs and PCNs in soils around a heavily industrialized area in Kocaeli, Turkey: concentrations, distributions, sources and toxicological effects *Sci. Total Environ.* **560–561** 160–9

Cetin B, Yurdakul S, Gungormus E, Ozturk F and Sofuoglu S C 2018 Source apportionment and carcinogenic risk assessment of passive air sampler-derived PAHs and PCBs in a heavily industrialized region *Sci. Total Environ.* **633** 30–41

Ceylan R F, Sayin C, Mencet Yelboğa M N, Özalp M, Ilbasmiş E and Sav O 2018 Land ownership and profitability of greenhouse production: antalya case *Turkish J. Agric. Food Sci. Technol.* **6** 930–5

Chai C, Cheng Q, Wu J, Zeng L, Chen Q, Zhu X, Ma D and Ge W 2017 Contamination, source identification, and risk assessment of polycyclic aromatic hydrocarbons in the soils of vegetable greenhouses in Shandong, China *Ecotoxicol. Environ. Saf.* **142** 181–8

Chakraborty P, Selvaraj S, Nakamura M, Prithiviraj B, Cincinelli A and Bang J J 2018 PCBs and PCDD/Fs in soil from informal e-waste recycling sites and open dumpsites in India: levels, congener profiles and health risk assessment *Sci. Total Environ.* **621** 930–8

Chakraborty P, Zhang G, Li J, Selvaraj S, Breivik K and Jones K C 2016 Soil concentrations, occurrence, sources and estimation of air–soil exchange of polychlorinated biphenyls in Indian cities *Sci. Total Environ.* **562** 928–34

Ciarkowska K, de Carvalho M and Gambus F 2022 Analysis of polycyclic aromatic hydrocarbons (PAHs) sources and vertical distribution in soils of the age-diverse brownfields of southern Poland using positive matrix factorisation and data mining model *Sustainability* **14** 13796

Combi T, Miserocchi S, Langone L and Guerra R 2016 Polychlorinated biphenyls (PCBs) in sediments from the western Adriatic Sea: sources, historical trends and inventories *Sci. Total Environ.* **562** 580–7

Devi N L, Yadav I C, Shihua Q, Dan Y, Zhang G and Raha P 2016 Environmental carcinogenic polycyclic aromatic hydrocarbons in soil from Himalayas, India: implications for spatial distribution, sources apportionment and risk assessment *Chemosphere* **144** 493–502

Dorais M, Papadopoulos A P and Gosselin A 2000 *Greenhouse Tomato Fruit Quality* (*Horticultural Reviews* 26) (Wiley) 239–319

Dumanoglu Y, Gaga E O, Gungormus E, Sofuoglu S C and Odabasi M 2017 Spatial and seasonal variations, sources, air-soil exchange, and carcinogenic risk assessment for PAHs and PCBs in air and soil of Kutahya, Turkey, the province of thermal power plants *Sci. Total Environ.* **580** 920–35

Eckhardt S, Breivik K, Manø S and Stohl A 2007 Record high peaks in PCB concentrations in the Arctic atmosphere due to long-range transport of biomass burning emissions *Atmos. Chem. Phys.* **7** 4527–36

Ediagbonya T F, Rotimi O M, Elumah O F and Pere J V 2025 Polychlorinated biphenyls contamination in Nigeria Soils: a risk assessment study in South-West and South-South, Regions *Earth Syst. Environ.* **9** 1215–33

Emoyan O O, Peretiemo-clarke B O, Tesi G O, Ohwo E and Adjerese W 2022 Concentrations, sources, and associated risks of polychlorinated biphenyls measured in soil profiles from selected telecom-masts in the Niger Delta, Nigeria *Soil Sediment Contam.* **31** 293–315

EPA 1989 Risk assessment guidance for superfund. Volume I: human health evaluation manual (part a) EPA/540/1–89/002 (available at: www.epa.gov/risk/risk-assessment-guidance-superfund-rags-part)

Hopke P K 2016 Review of receptor modeling methods for source apportionment *J. Air Waste Manag. Assoc.* **66** 237–59

Hu X, Zhu J and Ding Q 2011 Environmental life-cycle comparisons of two polychlorinated biphenyl remediation technologies: incineration and base catalyzed decomposition *J. Hazard. Mater.* **191** 258–68

Jahnke J C and Hornbuckle K C 2019 PCB emissions from paint colorants *Environ. Sci. Technol.* **53** 5187–94

Karaca C 2023 Estimation of daily global solar radiation based on different whitening applications using temperature in mediterranean type greenhouses *Ital. J. Agrometeorol.* **1** 79–93

Khalili N R, Scheff P A and Holsen T M 1995 PAH source fingerprints for coke ovens, diesel and, gasoline engines, highway tunnels, and wood combustion emissions *Atmos. Environ.* **29** 533–42

Kilunga P I, Sivalingam P, Laffite A, Grandjean D, Mulaji C K, de Alencastro L F, Mpiana P T and Poté J 2017 Accumulation of toxic metals and organic micro-pollutants in sediments from tropical urban rivers, Kinshasa, Democratic Republic of the Congo *Chemosphere* **179** 37–48

Kurt-Karakus P B *et al* 2018 The first countrywide monitoring of selected POPs: polychlorinated biphenyls (PCBs), polybrominated diphenyl ethers (PBDEs) and selected organochlorine pesticides (OCPs) in the atmosphere of Turkey *Atmos. Environ.* **177** 154–65

Lee R G M, Coleman P, Jones J L, Jones K C and Lohmann R 2005 Emission factors and importance of PCDD/Fs, PCBs, PCNs, PAHs and PM_{10} from the domestic burning of coal and wood in the U.K *Environ. Sci. Technol.* **39** 1436–47
Li T, Hu J, Xu C and Jin J 2023 PCBs, PCNs, and PCDD/Fs in soil around an industrial park in northwest china: levels, source apportionment, and human health risk *Int. J. Environ. Res. Public Health* **20** 3478
Mamontova E A, Tarasova E N, Mamontov A A, Kuzmin M I, McLachlan M S and Khomutova M I 2007 The influence of soil contamination on the concentrations of PCBs in milk in Siberia *Chemosphere* **67** S71–S78
Maraveas C 2019 Environmental sustainability of greenhouse covering materials *Sustainability* **11** 6129
Meijer S N, Ockenden W A, Sweetman A, Breivik K, Grimalt J O and Jones K C 2003 Global distribution and budget of PCBs and HCB in background surface soils:implications for sources and environmental processes *Environ. Sci. Technol.* **37** 667–72
Nisbet I C T and LaGoy P K 1992 Toxic equivalency factors (TEFs) for polycyclic aromatic hydrocarbons (PAHs) *Regul. Toxicol. Pharmacol.* **16** 290–300
Norris G, Duvall R, Brown S and Bai S 2014 EPA positive matrix factorization 5.0 fundamentals and user guide (available at: www.epa.gov/air-research/epa-positive-matrix-factorization-50-fundamentals-and-user-guide) (Accessed 04 05 2026)
Odabasi M, Dumanoglu Y, Ozgunerge Falay E, Tuna G, Altiok H, Kara M, Bayram A, Tolunay D and Elbir T 2016 Investigation of spatial distributions and sources of persistent organic pollutants (POPs) in a heavily polluted industrial region using tree components *Chemosphere* **160** 114–25
Olgun B and Doğan G 2020 Polycyclic aromatic hydrocarbon concentrations in soils of greenhouses located in Aksu Antalya, Turkey *Water Sci. Technol.* **81** 283–92
Paatero P and Tapper U 1994 Positive matrix factorization—a nonnegative factor model with optimal utilization of error-estimates of data values *Environmetrics* **5** 111–26
Perendeci N A, Gökgöl S and Orhon D 2018 Impact of alkaline H_2O_2 pretreatment on methane generation potential of greenhouse crop waste under anaerobic conditions *Molecules* **23** 1794
Perraudin E, Budzinski H and Villenave E 2007 Kinetic study of the reactions of ozone with polycyclic aromatic hydrocarbons adsorbed on atmospheric model particles *J. Atmos. Chem.* **56** 57–82
Ravindra K, Sokhi R and Van Grieken R 2008 Atmospheric polycyclic aromatic hydrocarbons: source attribution, emission factors and regulation *Atmos. Environ.* **42** 2895–921
Reff A, Eberly S I and Bhave P V 2007 Receptor modeling of ambient particulate matter data using positive matrix factorization: review of existing methods *J. Air Waste Manag. Assoc.* **57** 146–54
Salihoglu G, Salihoglu N K, Aksoy E and Tasdemir Y 2011 Spatial and temporal distribution of polychlorinated biphenyl (PCB) concentrations in soils of an industrialized city in Turkey *J. Environ. Manage.* **92** 724–32
Scarascia-Mugnozza G, Sica C and Russo G 2011 Plastic materials in European agriculture: actual use and perspectives *J. Agric. Eng.* **42** 15–28
Simcik M F, Eisenreich S J and Lioy P J 1999 Source apportionment and source/sink relationships of PAHs in the coastal atmosphere of Chicago and Lake Michigan *Atmos. Environ.* **33** 5071–9
Tsai W 2010 Current status and regulatory aspects of pesticides considered to be persistent organic pollutants (POPs) in Taiwan *Int. J. Environ. Res. Public Health* **7** 3615–27
TUIK 2026 Crop production statistics (available at: https://biruni.tuik.gov.tr/medas/?kn=92&locale=en)
U.S. EPA 2011 *Exposure Factors Handbook 2011 Edition (Final Report)* (available at: https://assessments.epa.gov/risk/document/&deid=236252#downloads)
Van den Berg M *et al* 2006 The 2005 world health organization reevaluation of human and mammalian toxic equivalency factors for dioxins and dioxin-like compounds *Toxicol. Sci.* **93** 223–41
Vane C H, Kim A W, Beriro D J, Cave M R, Knights K, Moss-hayes V and Nathanail P C 2014 Polycyclic aromatic hydrocarbons (PAH) and polychlorinated biphenyls (PCB) in urban soils of Greater London, UK *Appl. Geochem.* **51** 303–14
von Elsner B, Briassoulis D, Waaijenberg D, Mistriotis A, von Zabeltitz C, Gratraud J, Russo G and Suay-cortes R 2000 Review of structural and functional characteristics of greenhouses in European Union countries: part I, design requirements *J. Agric. Eng. Res.* **75** 1–16
Wang D, Ma J, Li H and Zhang X 2018 Concentration and potential ecological risk of PAHs in different layers of soil in the petroleum-contaminated areas of the loess plateau, China *Int. J. Environ. Res. Public Health* **15** 1785
Wang P, Zhang Q, Wang Y, Wang T, Li X, Li Y, Ding L and Jiang G 2009 Altitude dependence of polychlorinated biphenyls (PCBs) and polybrominated diphenyl ethers (PBDEs) in surface soil from Tibetan Plateau, China *Chemosphere* **76** 1498–504
Wang S, Ni H-G, Sun J-L, Jing X, He J-S and Zeng H 2013 Polycyclic aromatic hydrocarbons in soils from the Tibetan Plateau, China: distribution and influence of environmental factors *Environ. Sci. Process. Impacts* **15** 661–7
Wilcke W 2007 Global patterns of polycyclic aromatic hydrocarbons (PAHs) in soil *Geoderma* **141** 157–66
Wu S, Xia X, Yang L and Liu H 2011 Distribution, source and risk assessment of polychlorinated biphenyls (PCBs) in urban soils of Beijing, China *Chemosphere* **82** 732–8
Xing Y, Lu Y, Dawson R W, Shi Y, Zhang H, Wang T, Liu W and Ren H 2005 A spatial temporal assessment of pollution from PCBs in China *Chemosphere* **60** 731–9
Yang W, Lang Y and Li G 2014 Concentration, source, and carcinogenic risk of PAHs in the soils from Jiaozhou Bay Wetland *Polycycl. Aromat. Compd.* **34** 439–51
Yao M, Li Z, Zhang X and Lei L 2014 Polychlorinated biphenyls in the centralized wastewater treatment plant in a chemical industry zone: source, distribution, and removal *J. Chem.* **2014** 1–10
Yurdakul S, Çelik I, Çelen M, Öztürk F and Cetin B 2019 Levels, temporal/spatial variations and sources of PAHs and PCBs in soil of a highly industrialized area *Atmos. Pollut. Res.* **10** 1227–38
Zaimoglu Z and Baytorun N 2018 Climate control in mediterranean greenhouses A Shanker, C Shanker and C Srinivasarao ed *Climate Resilient Agriculture—Strategies and Perspectives* (IntechOpen) (https://doi.org/10.5772/intechopen.72367)
Zhang X *et al* 2021 Assessing approaches of human inhalation exposure to polycyclic aromatic hydrocarbons: a review *Int. J. Environ. Res. Public Health* **18** 3124
Zhang X, Song X, Zhang H, Hou Y, Li Y and Zhao X 2025 Source apportionment and human health risk assessment of polycyclic aromatic hydrocarbons in vegetable greenhouse soils in Shenyang, China *Water, Air, & Soil Pollution* **236** 435

Zhang Y, Niu J, Wei Z, Zhou X, Wu L, Li X, Ma S and Shi G 2023 Spatial distribution characteristics, source analysis and risk assessment of polycyclic aromatic hydrocarbons in topsoil of a typical chemical industry park *Front. Environ. Sci.* **11** 1209137

Zheng X, Liu X, Jiang G, Wang Y, Zhang Q, Cai Y and Cong Z 2012 Distribution of PCBs and PBDEs in soils along the altitudinal gradients of Balang Mountain, the east edge of the Tibetan Plateau *Environ. Pollut.* **161** 101–6

Zhu X, Fan Z, Wu X, Jung K H, Ohman-strickland P, Bonanno L J and Lioy P J 2011 Ambient concentrations and personal exposure to polycyclic aromatic hydrocarbons (PAH) in an urban community with mixed sources of air pollution *J. Expo. Sci. Environ. Epidemiol.* **21** 437–49